Journal of Physiology (2002), **542.2**, *pp.* 567–581
DOI: 10.1113/jphysiol.2002.019059

www.jphysiol.org

Synchronized oscillations caused by disinhibition in rodent neocortex are generated by recurrent synaptic activity mediated by AMPA receptors

Manuel A. Castro-Alamancos and Pavlos Rigas

Department of Neurology and Neurosurgery, Montreal Neurological Institute, McGill University, Montreal, Quebec, Canada H3A 2B4

During disinhibition the neocortex generates synchronous activities. In neocortical slices application of $GABA_A$ and $GABA_B$ receptor antagonists transformed slow oscillations into large amplitude spike–wave discharges that contained a rhythmic ~10 Hz neocortical oscillation. The 10 Hz oscillations caused by disinhibition were highly region specific and were generated only in frontal agranular regions of neocortex, such as the primary motor cortex, but not in granular neocortex. Pharmacological manipulations showed that the 10 Hz oscillations were critically dependent on α-amino-3-hydroxy-5-methylisoxazole-4-propionate (AMPA) receptors. Current source density (CSD) analyses in slices using 16-site silicon probes revealed that the 10 Hz oscillations were expressed with large current sinks in the upper layers and smaller current sinks in the lower layers that precede them. The results indicate that blocking $GABA_B$ receptors in the agranular neocortex unmasks recurrent synaptic activity mediated by AMPA receptors that results in the generation of these oscillations.

(Resubmitted 17 February 2002; accepted after revision 8 April 2002)
Corresponding author M. A. Castro-Alamancos: Room WB210, Montreal Neurological Institute, 3801 University Street, Montreal, Quebec, Canada H3A 2B4. Email: mcastro@bic.mni.mcgill.ca

Early studies in cats have shown that application of the $GABA_A$ receptor antagonist penicillin in neocortex results in the production of synchronous activity consisting of a negative spike followed by a positive wave that recurs continually every 1–3 s (1–0.33 Hz) (Ralston, 1958; Matsumoto & Ajmone-Marsan, 1964; Gloor *et al.* 1977). Work *in vitro* using neocortical slices has also shown that application of the $GABA_A$ receptor antagonist bicuculline (BMI) produces synchronized activity in adult neocortex (Gutnick *et al.* 1982; Connors, 1984). However, a major difference between the activity generated in adult slices and *in vivo* is that the activity in slices does not recur periodically, and must be normally triggered by orthodromic stimulation, unless immature slices are used (Hablitz, 1987). One reason for this difference may be that the neocortex of control slices in those studies did not generate spontaneous slow oscillations, like the neocortex of anaesthetized or sleeping animals (Steriade *et al.* 1993, 1996). Recent work *in vitro* has shown that modifying the traditional buffer used to bath slices produces spontaneous activity in neocortex that resembles slow oscillations (Sanchez-Vives & McCormick, 2000). Thus, the first aim of the present study is to investigate the effects of $GABA_A$ receptor blockade in neocortical slices that produce slow oscillations in control conditions.

Blocking $GABA_A$ and $GABA_B$ receptors (disinhibition) in the primary motor neocortex of anaesthetized rats transforms cortical slow wave oscillations into large amplitude discharges that consist of a large negative spike followed by five to fifteen low amplitude negative spikes that form a rhythmic ~10 Hz (7–14 Hz) oscillation (Castro-Alamancos, 2000). These 10 Hz neocortical oscillations caused by disinhibition were shown to be of cortical origin and could originate in the upper or lower layers but they always propagated to the same location in upper layer V–IV. This was true for the first negative spike in the discharge but not for the low amplitude negative spikes that follow and form the 10 Hz oscillations. The low amplitude negative spikes that form the 10 Hz oscillation always originate in lower layer V–VI and do not spread to upper layer V–IV, jumping instead directly to the upper layers (Castro-Alamancos, 2000). In anaesthetized cats, repetitive discharges similar to the 10 Hz oscillations observed in rats occur sporadically after $GABA_A$ receptor blockade and are called 'afterdischarges' (Ralston, 1958) or 'fast-runs' when they are longer lasting (Steriade *et al.* 1998). Afterdischarges similar to those observed in the neocortex have also been described and investigated in the hippocampus *in vitro* and *in vivo* (Miles *et al.* 1984; Hablitz, 1984; Lee & Hablitz, 1990; Traub *et al.* 1993*a, b*, 1996; Bragin *et al.* 1997*a*, *b*). Activity similar to the 10 Hz oscillations and afterdischarges observed *in vivo* has been observed in adult neocortical slices bathed with low magnesium buffers (Silva *et al.* 1991), but never after disinhibition. Thus, the second aim of the present study is to investigate the effect of disinhibition ($GABA_A$ and $GABA_B$ receptor blockade) in spontaneously active neocortical slices.

The results show that disinhibition induces 10 Hz oscillations in agranular, but not granular neocortex. Pharmacological manipulations demonstrate that blocking AMPA receptors, but not any other glutamate receptor, completely abolishes the 10 Hz oscillations leaving intact the spike–wave discharges caused by blocking $GABA_A$ receptors alone. Finally, current source density (CSD) analysis reveals that the 10 Hz oscillations are strongly expressed in the upper layers, perhaps as a result of preceding activity in the lower layers.

METHODS

Slices were prepared from adult (⩾7 weeks) BALB/C mice according to the methods described by Agmon & Connors (1991). Mice were deeply anaesthetized with sodium pentobarbitone (60 mg kg^{-1}) and upon losing all responsiveness to a strong tail pinch the brain was rapidly extracted and placed in ice-cold buffer solution (ACSF, see below). Slices (400 μm thick) were cut in ice-cold buffer solution using a vibratome. Six sequential slices were taken from each animal (see Fig. 2*A*). During the experiments living slices were photographed with a CCD camera to assure the location of recording sites. Experiments were performed in an interface chamber at 32 °C. The slices were bathed constantly (1–1.5 ml min^{-1}) with artificial cerebrospinal fluid (ACSF) containing (mM): NaCl 126, KCl 3.5, NaH_2PO_4 1.25, $NaHCO_3$ 26, $MgSO_4.7H_2O$ 1.3, dextrose 10, $CaCl_2.2H_2O$ 1.2. The ACSF was bubbled with 95 % O_2–5 % CO_2. This ACSF composition has been shown to produce spontaneous slow oscillations in neocortical slices that are similar to those observed in the neocortex of anaesthetized animals *in vivo* (Sanchez-Vives & McCormick, 2000). Field recordings were made using low-impedance pipettes (~0.5 MΩ) filled with ACSF or using linear 16-channel silicon probes with 100 μm inter-site spacing (Center for Neural Communication Technology, University of Michigan) as previously described (Castro-Alamancos, 1999, 2000). Intracellular recordings were performed using high-impedance (80–100 MΩ) pipettes filled with potassium acetate (2–3 M). All procedures were reviewed and approved by the Animal Care Committee of McGill University.

RESULTS

Neocortical synchronized oscillations induced by disinhibition *in vitro*

Previous work *in vivo* has shown that disinhibition produces synchronized oscillations at ~10 Hz in the frontal agranular neocortex (i.e. primary motor cortex) (Castro-Alamancos, 2000). In the present study *in vitro*, recordings were initially performed in the upper layers (layer III) of slices from the same area, the frontal agranular neocortex (unless otherwise indicated). Field potential recordings in control conditions revealed the occurrence of small amplitude spontaneous events resembling the slow oscillatory activity observed *in vivo* in anaesthetized animals (Fig. 1*A*). These events occurred at a frequency of 0.12 ± 0.03 Hz (mean ± S.D.; $n = 10$ slices) and their amplitude was 0.24 ± 0.02 mV. Application of a $GABA_A$ receptor antagonist (bicuculline methobromide, BMI; 10 μM) transformed the small amplitude low frequency events into large amplitude discharges consisting of a negative spike followed by a positive wave (Fig. 1*A*). The discharges occurred spontaneously at 0.1 ± 0.02 Hz and

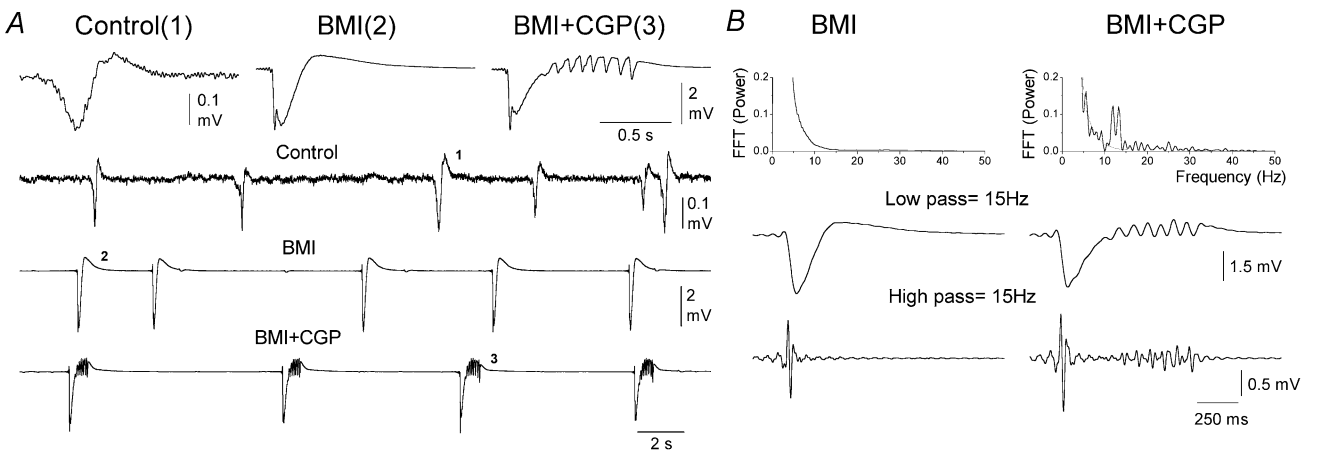

Figure 1. Spontaneous activity in agranular neocortex slices during control conditions and during disinhibition

A, examples of field potential recordings from layer III of agranular neocortex during control conditions (Control), during subsequent application of the $GABA_A$ receptor antagonist bicuculline (BMI, 10 μM) and during application of BMI plus the $GABA_B$ receptor antagonist CGP35348 (BMI+CGP, 10+500 μM). The upper traces show single numbered events, on an expanded time scale, taken from corresponding points on the continuous recording shown below. *B*, power spectrum analysis of spontaneous activities induced by disinhibition in agranular neocortex. Upper panel, fast Fourier transforms (FFT) of a representative discharge induced by BMI (left) and by BMI plus CGP35348 (right). In the right panel the two FFTs are overlaid for comparison. Lower panels, digital filtering of the representative discharges. Low-pass filtering at 15 Hz and high-pass filtering at 15 Hz.

their amplitude was 2.9 ± 0.4 mV (n = 10 slices). Furthermore, addition of a $GABA_B$ receptor antagonist (CGP35348; 500 μM) transformed the large amplitude discharges caused by BMI into a large amplitude negative spike followed by three to fifteen low amplitude negative spikes at ~10 Hz (Fig. 1*A*). These discharges, which for simplicity we call 10 Hz oscillations, occurred spontaneously at a frequency of 0.07 ± 0.02 Hz (n = 10 slices).

To characterize the activities produced by disinhibition a power spectrum analysis was performed on the characteristic discharges generated by $GABA_A$ and $GABA_B$ receptor antagonists (Fig. 1*B*). Fast Fourier transforms reveal that the 10 Hz oscillations caused by BMI+CGP35348 and the discharges produced by BMI alone differed primarily in that the 10 Hz oscillations had a large power component between 10 and 15 Hz, as well as the occurrence of smaller components above 15 Hz (Fig. 1*B*). Digital filtering of the raw signal reveals that the low frequency range, up to 15 Hz (Fig. 1*B*), consisted of a large amplitude initial negative spike, which was followed by an oscillation when $GABA_B$ receptors were blocked. Furthermore, at frequencies above 15 Hz the event generated with $GABA_A$ receptor blockade consisted of a population spike at the onset of the discharge, while the $GABA_B$ receptor blockade also produced a series of smaller population spikes close to

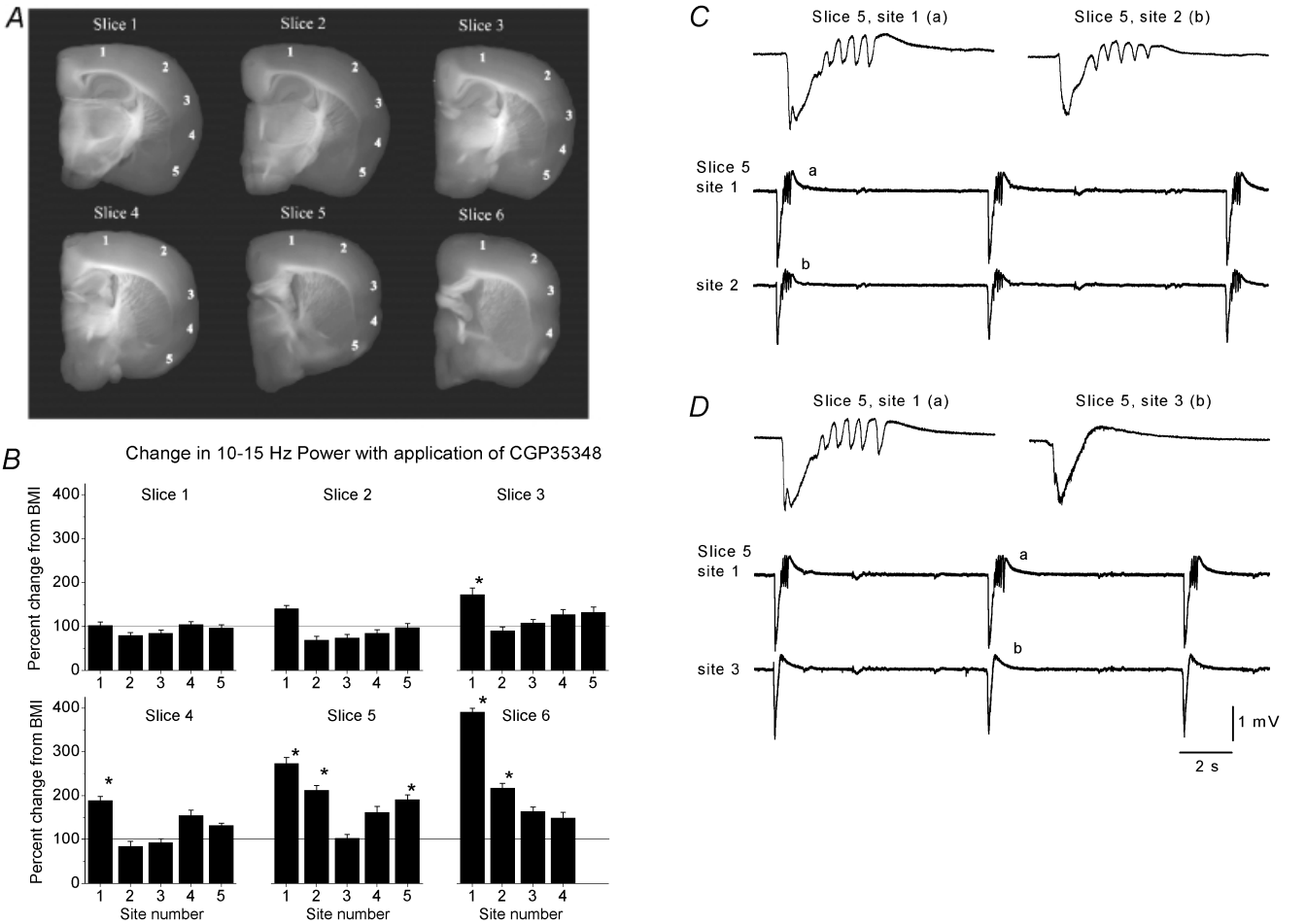

Figure 2. Region specificity of 10 Hz synchronized oscillations

A, six representative slices cut in the thalamocortical plane and taken sequentially from caudal (slice 1) to most rostral (slice 6). The numbers on each slice (1–5) mark the location where the recordings were performed. *B*, recordings were performed in slices bathed with BMI before and during the application of CGP35348. The plots show the percentage change in the 10–15 Hz power range after application of CGP35348 for every recording site and slice shown above. The data are means ± S.D. from n = 6 experiments (36 slices). Asterisks indicate a significant change with respect to BMI alone. Note the enhancement in 10–15 Hz power in sites 1 and 2 of slices 5 and 6. *C*, simultaneous field potential recordings from sites 1 and 2 of slice 5 as shown in *A* during application of BMI+CGP35348. Note the occurrence of 10 Hz oscillations in both sites. *D*, subsequent positioning of the recording electrode from site 2 to 3 reveals that site 3 does not express 10 Hz oscillations but only a discharge consisting of a large amplitude negative spike followed by a positive wave, while site 1 continues to produce 10 Hz oscillations. The letters on the single events shown on the upper traces correspond to the events shown below on the continuous recordings.

the offset of the oscillation (Fig. 1*B*). In conclusion, blocking $GABA_B$ receptors in the frontal agranular neocortex *in vitro* transforms large amplitude spike and wave discharges caused by blocking $GABA_A$ receptors into ~10 Hz oscillations.

Cortical region specificity of synchronized oscillations

The present experiments *in vitro* and previous work *in vivo* (Castro-Alamancos, 2000) have shown that disinhibition produces synchronized 10 Hz oscillations in the frontal neocortex (i.e. agranular primary motor cortex area). However, the cortex is formed of a collection of functionally and structurally diverse regions, from sensory to motor to associative. Thus, the next experiments explored the effects of disinhibition in different cortical regions. In each of these experiments six slices were taken sequentially and multiple sites from those slices were monitored during $GABA_A$ receptor blockade and during $GABA_A$ plus $GABA_B$ receptor blockade (Fig. 2*A*). Slice 1 was the most caudal slice obtained and slice 6 was the most rostral slice. Recordings were obtained with two ACSF-filled pipettes. For each slice, one recording electrode was placed in site 1, while the other electrode was moved from sites 2 to 5. The site 1 recording electrode assured that the activity in the slice was constant while recording was performed in the other sites. In order to obtain a measure of the capability of different cortical regions to produce 10 Hz oscillations during disinhibition a power spectrum analysis was calculated on ten spontaneous discharges per recording site in slices bathed with a $GABA_A$ receptor antagonist (BMI; 10 μM) before and during the application of a $GABA_B$ receptor antagonist (CGP35348; 500 μM). Figure 2*B* shows the percentage change in power between 10 and 15 Hz for each recorded site during application of the $GABA_B$ receptor antagonist (CGP35348; 500 μM; $n = 6$ experiments, i.e. 36 slices). Note that in the neocortex, only site 1 and 2 in slices 5 and 6 and site 1 in slices 3 and 4 developed a strong and significant increase (Fig. 2*B*; $P < 0.0001$, Student's t test) in the 10–15 Hz range reflecting the generation of 10 Hz oscillations in these sites. In addition, some sites in the piriform cortex also developed activity in this frequency range (site 5 in slice 5). These results reveal strong region specificity for the generation of 10 Hz oscillations caused by disinhibition. In particular, the frontal agranular neocortex and parts of the piriform cortex are capable of generating 10 Hz oscillations during disinhibition. Figure 2*C* shows simultaneous recordings from sites 1 and 2 of slice 5 in the presence of disinhibition ($GABA_A$ and $GABA_B$ block) and Fig. 2*D* shows simultaneous recordings from site 1 and 3 of the same slice also during disinhibition. Note that sites 1 and 2 show clear 10 Hz oscillations while site 3 does not. The present study will not deal further with the piriform cortex. In conclusion, the results indicate that there is a gradient in the generation of 10 Hz oscillations so that the frontal and agranular neocortex is capable of generating these oscillations while the posterior and granular neocortex does not generate them.

The slices used in the present study were cut in the thalamocortical plane, and thus a thalamic involvement in the 10 Hz activity described could be suggested. However, it is important to note that the slices that produce the 10 Hz oscillations (i.e. slices 4–6) do not contain connections between thalamus and cortex, and that the thalamocortical slices *per se* (i.e. slices 1–3) do not produce the 10 Hz oscillation. Finally, it is also noteworthy that the generation of 10 Hz oscillations in the agranular cortex is unaffected by isolating the cortex from all subcortical structures (not shown). This supports previous findings *in vivo* demonstrating a lack of involvement of the thalamus in the generation of 10 Hz oscillations caused by cortical disinhibition (Castro-Alamancos, 2000) and also fast-runs in cats (Steriade & Contreras, 1998).

Effects of metabotropic, NMDA and non-NMDA glutamate receptor antagonists on synchronized oscillations

The next experiments explored the receptors involved in generating 10 Hz oscillations in the frontal agranular neocortex. Since glutamate and GABA are the two major neurotransmitters in the neocortex (Somogyi *et al.* 1998), the 10 Hz oscillations necessarily involve glutamate receptors because both $GABA_A$ and $GABA_B$ receptors are blocked. Thus, to investigate the contribution of different types of glutamate receptors in the expression of 10 Hz oscillations we used metabotropic, NMDA and non-NMDA (AMPA/kainate) receptor blockers. Application of a metabotropic glutamate receptor antagonist (MCPG, 1 mM; $n = 3$ experiments) had little effect on the 10 Hz oscillations produced by disinhibition (not shown). Thus, the mean power at 10–15 Hz was not reduced by MCPG, but was actually slightly increased by 9 ± 2 %. Therefore, the generation and expression of 10 Hz oscillations does not require metabotropic glutamate receptors. In contrast, application of an NMDA receptor antagonist (APV; 100 μM; $n = 5$ experiments) had a significant effect on the 10 Hz oscillations. Figure 3*A* shows raw traces of 10 Hz oscillations produced by disinhibition, and the effects of an NMDA receptor antagonist 15 and 40 min after continuous application of 100 μM APV. Note that APV did not abolish the 10 Hz oscillations, but transformed them into higher frequency oscillations. Thus, in the presence of APV the small oscillatory events following the first large amplitude negative spikes were clearly present. However, the frequency of these small events increased and their amplitude was reduced. Figure 3*B* and *C* shows population data ($n = 5$ experiments) corresponding to a power spectrum analysis comparing events in the presence of a $GABA_A$ receptor antagonist (BMI), and a $GABA_A$ and

$GABA_B$ receptor antagonist (BMI+CGP) plus APV (BMI+CGP+APV). Note that APV indeed reduces the power components at 10–15 Hz, but at the same time it increases higher frequency components between 15 and 25 Hz. Thus, blocking NMDA receptors does not abolish the oscillations generated by disinhibition, it simply transforms them into higher frequency oscillations, which is consistent with the idea that NMDA receptors participate in the expression of these oscillations. In particular, these data indicate that NMDA receptors have an important role in shaping the frequency of the oscillation.

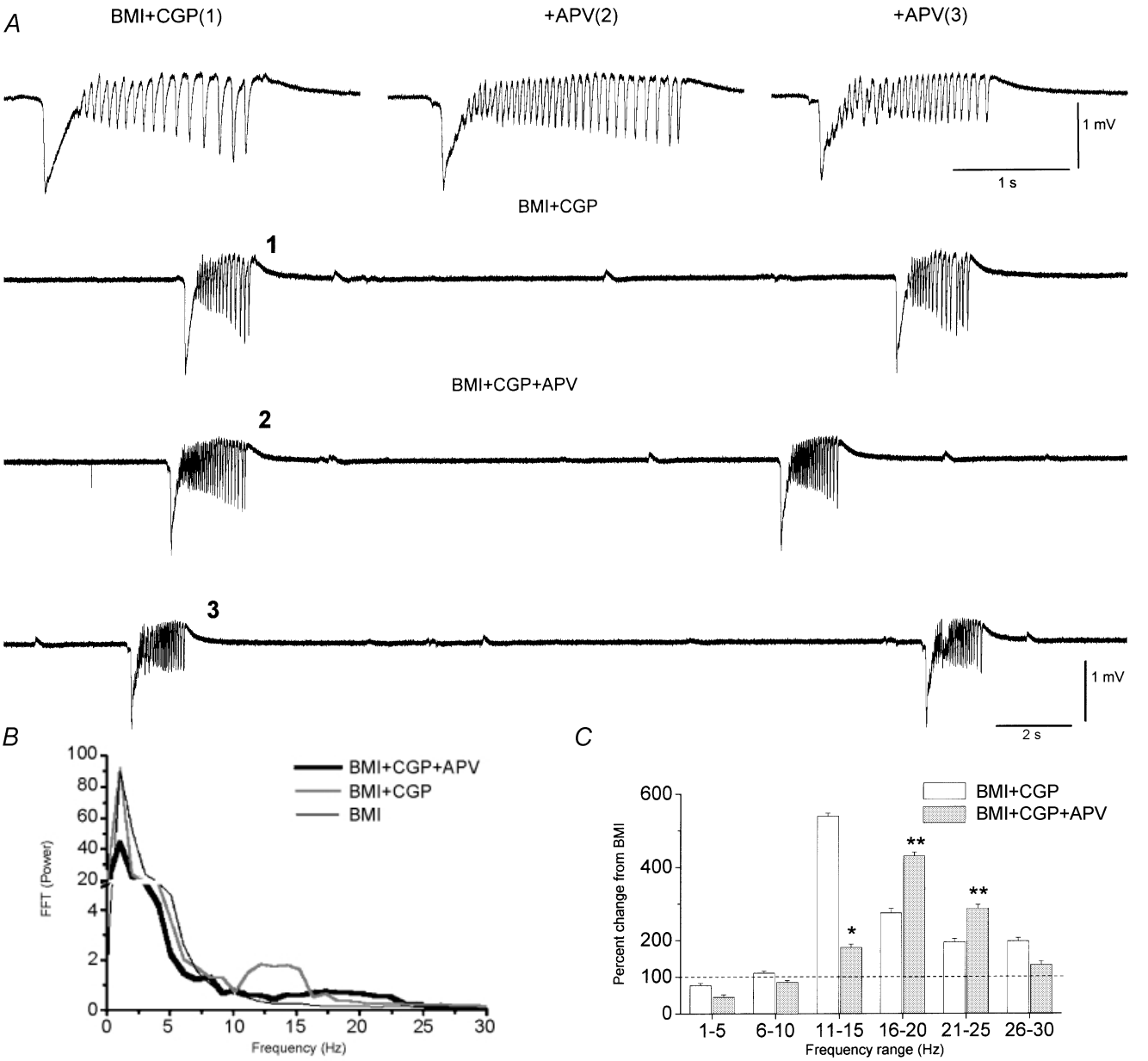

Figure 3. Effect of NMDA receptor block on spontaneous activity in agranular neocortex during disinhibition

A, examples of spontaneous field potential activity recorded during bath application of BMI plus CGP35348 (trace 1) and subsequent addition of APV (100 μM) (traces 2 and 3). The numbers on the upper single traces correspond to the activity shown below. The difference between 2 and 3 is the time after the beginning of APV application, which was 15 and 40 min, respectively. *B*, fast Fourier transform of single events recorded during BMI, BMI+CGP and BMI+CGP+APV (10 events per condition are averaged). Note the reduction in the power range between 10 and 15 Hz during application of APV and the simultaneous enhancement of the power range between 15 and 25 Hz. *C*, population data show a significant reduction in the power range between 10 and 15 Hz (*) with application of APV, but also a significant enhancement in the power range between 15 and 25 Hz (**) with APV. Data correspond to five experiments (10 events per condition) and are expressed as the percentage change from BMI alone.

The previous results show that metabotropic glutamate receptors have little relevance to 10 Hz oscillations generated by disinhibition and that NMDA receptors are involved in shaping the expression of these oscillations. However, none of these receptors are critical for the generation of the oscillations since they are present when these receptors are blocked. This suggests that non-NMDA receptors may have a more critical role in the generation of oscillatory events caused by disinhibition. To test this possibility a non-NMDA receptor (CNQX, 10 μM; $n = 6$) antagonist was applied. During application of 10 μM CNQX the amplitude of the first large amplitude negative spike in a discharge and the amplitude of the small amplitude events that follow were measured independently. Figure 4*A* shows such an experiment. As CNQX was applied to the interface chamber the small events that form the 10 Hz oscillations were rapidly and completely abolished (Fig. 4*A*, open squares). This occurs while the drug is having no significant effect on the large amplitude initial event (Fig. 4*A*, filled circles). It took several more minutes for the large amplitude event to start declining in amplitude until it was also completely abolished. Thus, as the concentration of CNQX rises in the interface chamber the initial part of the discharge that is affected by the drug is the 10 Hz oscillation. Later, the large amplitude negative spike is also abolished completely. The result was the same in every experiment using CNQX ($n = 6$) so that the 10 Hz oscillation was completely abolished 3.5 ± 0.3 min prior to any significant decline (>10 %) of the initial large amplitude negative spike. These results indicate that the 10 Hz oscillations are very sensitive to low doses of the non-NMDA receptor antagonist CNQX. One possible interpretation of these results is that the oscillations are mediated by the non-NMDA receptors that are blocked by low doses of CNQX. Indeed, CNQX is known to have between 3 and 6 times more selectivity for AMPA receptors than for kainate receptors (Lerma *et al.* 2001), suggesting that the 10 Hz oscillations caused by disinhibition in the frontal agranular cortex are critically dependent on AMPA receptors. It is also known that 10 μM CNQX blocks NMDA receptors in neocortex by acting on the glycine site of the NMDA receptor (Hablitz & Sutor, 1990). To study the involvement of AMPA receptors we tested the effect of a small dose of CNQX (2 μM), which does not block either kainate or NMDA receptors. Figure 4*B* shows the amplitude of the first large negative spike from spontaneous discharges (Fig. 4*B*, filled circles) and the amplitude of the small events that follow and form the oscillation (Fig. 4*B*, open squares). Application of CGP35348 induced the oscillation while subsequent application of a low dose of CNQX (2 μM) completely abolished the oscillation without any

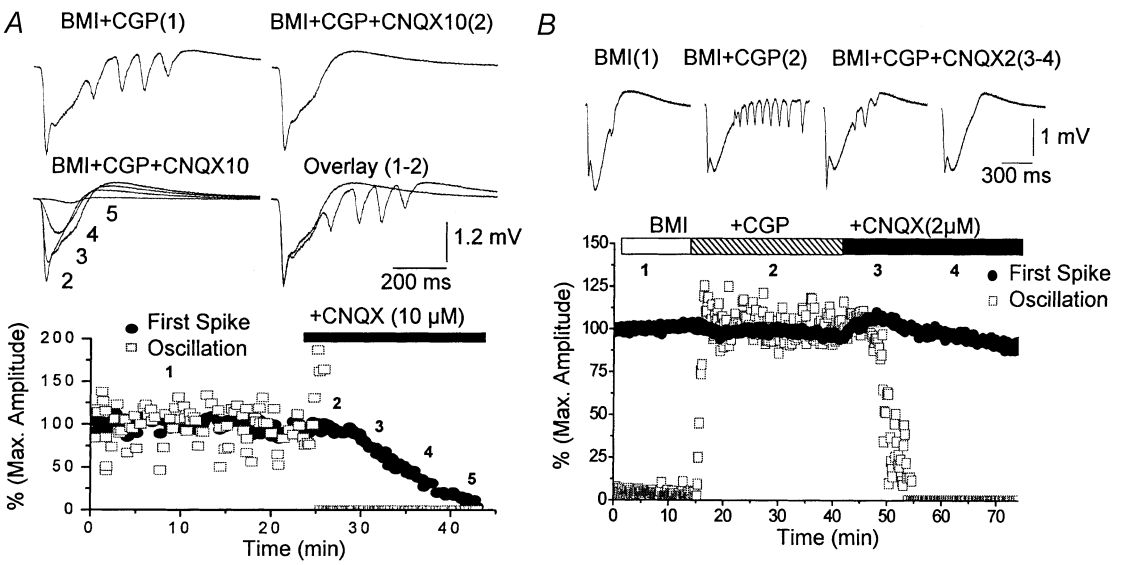

Figure 4. Effect of the non-NMDA receptor antagonist CNQX on 10 Hz oscillations induced by disinhibition

A, upper panel, representative traces corresponding to single spontaneous events produced during application of BMI+CGP35348 and at different times after starting application of CNQX (10 μM). The numbers on the traces correspond to the time shown below. Lower panel, effect of CNQX on the amplitude of the initial large amplitude negative spike (filled circles) and on the small amplitude spikes that follow and form the 10 Hz oscillations (open squares). For the small spikes the amplitude of the largest event among them was always used. Note the rapid abolition of the small amplitude spikes. *B*, upper panel, representative traces corresponding to single spontaneous events produced during application of BMI+CGP35348 and at different times after starting application of CNQX (2 μM). Lower panel, effect of CNQX on the amplitude of the initial large amplitude negative spike (filled circles) and on the small amplitude spikes that follow and form the 10 Hz oscillations (open squares). Note the selective abolishment of the oscillation.

significant effect on the first large amplitude negative spike. This result was obtained in every experiment ($n = 6$) so that the block of the 10 Hz oscillations was complete (100 %) while the first amplitude negative spike was reduced less than 10 % even after more than 1 h of application of CNQX (2 μM). In several cases ($n = 2$) subsequent application of the NMDA receptor antagonist APV (100 μM; not shown) completely eliminated the generation of the spontaneous discharges suggesting that synaptic activity mediated by NMDA receptors alone can sustain spontaneous discharges caused by blocking $GABA_A$ receptors (i.e. first large negative spike), but not the 10 Hz oscillations caused by blocking the $GABA_A$ and $GABA_B$ receptors.

In order to confirm that the effect of 2 μM CNQX was a selective block of AMPA receptors we tested the effect of a specific AMPA receptor antagonist GYKI53655. Application of GYKI53655 (15–30 μM; $n = 6$) produced the same effect on the 10 Hz oscillations as application of 2 μM CNQX, completely abolishing the oscillation with no significant effect on the initial large amplitude negative spike (not shown). This result was obtained in every experiment ($n = 6$) such that the block of the 10 Hz oscillations was complete (100 %) while the first amplitude negative spike was reduced less than 10 %. In conclusion, the present results show that the 10 Hz oscillations caused by disinhibition in the frontal agranular neocortex are critically dependent on AMPA receptors for their generation and expression. In addition, NMDA receptors are involved in the expression of 10 Hz oscillations and mainly serve to shape their frequency, so that when NMDA receptors are blocked the expression of the oscillation is transformed to a higher frequency.

Intracellular correlates of synchronized oscillations

The previous experiments demonstrate that blocking AMPA receptors completely eliminates the 10 Hz oscillations generated by disinhibition, while having little effect on the first large amplitude negative spike preceding the oscillations. This indicates that recurrent synaptic activity mediated by AMPA receptors is essential for the generation or expression of the 10 Hz oscillations. If AMPA receptors are only essential for the expression of

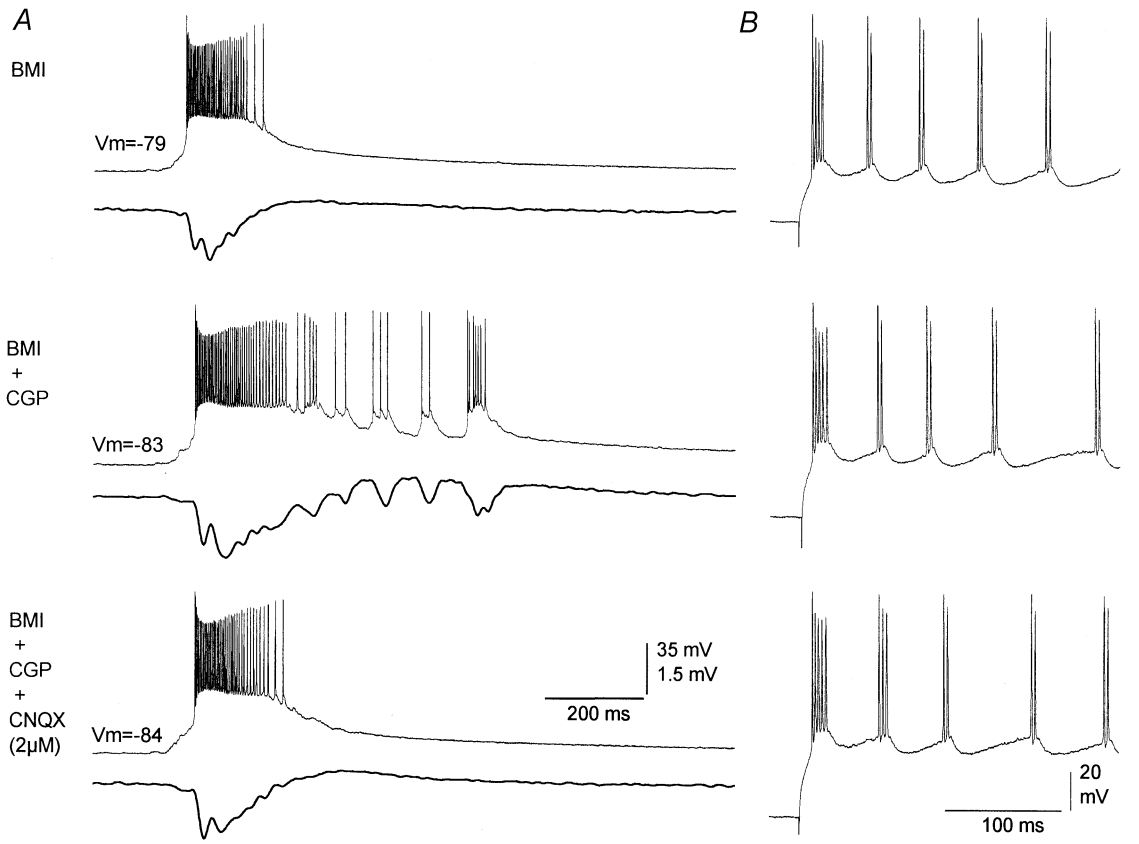

Figure 5. Effect of 2 μM CNQX on oscillations recorded from individual neurons

A, representative trace pairs of intracellular (layer V; upper trace) and extracellular (layer III; lower trace) recordings corresponding to spontaneous discharges produced during application of BMI, BMI+CGP35348 and BMI+CGP35348+CNQX (2 μM). Note the abolishment of the oscillation both at the intracellular and extracellular levels with CNQX. *B*, effect of an intracellular current pulse applied to the cell shown in *A* during the three pharmacological conditions. Note that there were no significant changes in the intrinsic repetitive pattern of discharge.

these oscillations it should be possible to observe individual cells that repetitively discharge at ~10 Hz with each spontaneous discharge after blocking these receptors. For example, layer V repetitive bursting cells would continue to produce spontaneous repetitive bursts, although asynchronously, with each discharge after application of 2 μM CNQX. Thus, the block of AMPA receptors would impede synchronization between cells and also the synaptic expression of this activity. Alternatively, AMPA receptors may be critical for the generation of the 10 Hz oscillations via recurrent synaptic connections. In this case all cells, including those that intrinsically burst repetitively at ~10 Hz, should cease to generate 10 Hz oscillations with each spontaneous discharge, although the intrinsic bursting cells should still produce repetitive burst with current injection. Recordings were performed from layer V neurons of neocortex (n = 15), which robustly express these oscillations as previously shown *in vivo* (Castro-Alamancos, 2000). Figure 5 shows such an experiment, performed in an intrinsically bursting cell in layer V and the corresponding field potential recording from the upper layers. Application of CGP35348 in the presence of BMI transformed the spontaneous discharges, consisting of a paroxysmal depolarizing shift (PDS), into a discharge followed by an oscillation at ~10 Hz (Fig. 5*A*). Subsequent application of CNQX (2 μM) had little effect on the initial

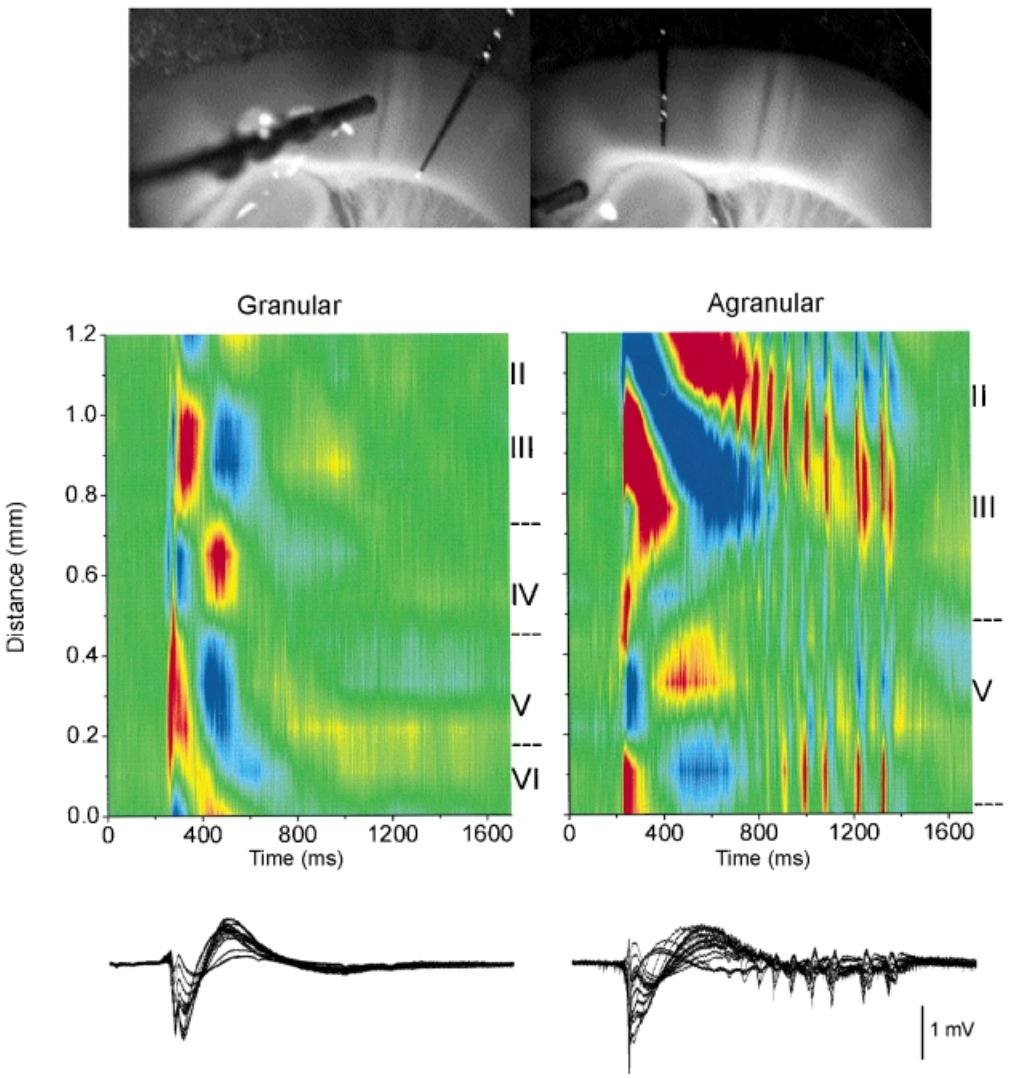

Figure 6. CSD analysis of spontaneous discharges recorded during disinhibition in granular and agranular regions of the same slice

Upper panel, photomicrographs of the slice preparation taken during the experiment showing the location of the 16-channel silicon probe used to derive the CSD analyses shown below. A lesion separated the granular and agranular regions. A stimulating electrode (shown in left panel) served to demonstrate the effectiveness of the lesion to eliminate communication between both regions by stimulating in one region and recording in the other. Middle panel, CSD analyses of spontaneous events recorded in the granular (left) and agranular (right) region of the same slice during BMI+CGP35348. Lower panel, the field potential recordings used to derive the CSD are overlaid. Current sinks are in red, sources are blue and zero is green.

spontaneous PDS discharge, but completely eliminated the 10 Hz oscillations in every cell. However, the intrinsic response of the neurons to current injection was not modified during the experiment so that the neurons continued to discharge repetitively in response to current injection throughout the experiment and under all pharmacological conditions (Fig. 5*B*). Thus, after application of 2 μM CNQX none of the neurons that we recorded from would spontaneously oscillate at 10 Hz with each PDS. This indicates that the 10 Hz oscillations cannot be explained simply as the synaptic manifestation of the intrinsic firing of layer V neurons. Indeed, synaptic coupling via AMPA receptors is critical for the generation of these oscillations.

Laminar origin of synchronized oscillations

The next experiments investigated the laminar profiles of the activities generated in the neocortex during disinhibition. Since the effects of disinhibition are highly region specific we compared the laminar profiles of activities generated in different regions of neocortex. In particular, the granular and agranular neocortex were

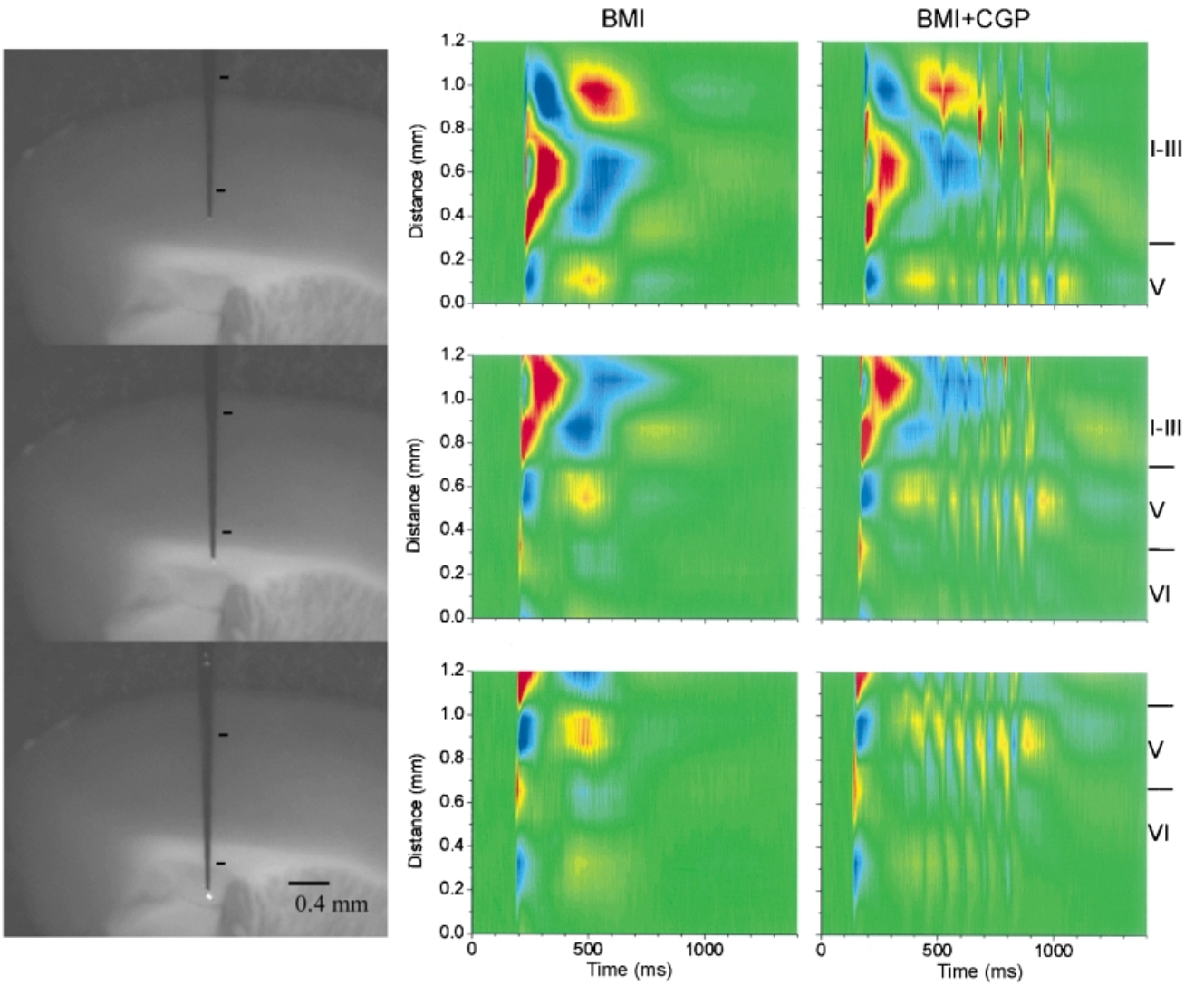

Figure 7. CSD analysis of spontaneous discharges in agranular neocortex during BMI and during BMI+CGP35348

Left panels, photomicrographs of the slice preparation taken during the experiment showing the location of the 16-channel silicon probe used to derive the CSD analyses in the middle and right panels. The marks indicate the region corresponding to the CSD area. Middle panels, CSD analysis corresponding to spontaneous discharges generated in the agranular cortex during application of BMI. Each CSD analysis corresponds to a single spontaneous discharge recorded in the same cortical area; the only difference is the distance of the probe with respect to the pia mater. CSD analyses were derived from the spontaneous activity without averaging. Right panels, CSD analysis corresponding to spontaneous discharges generated in the agranular cortex during application of BMI+CGP35348, and recorded in the same locations as in the middle panels.

compared using 16-site linear array silicon probes (100 μm inter-site spacing) placed on slices of neocortex *in vitro* (Fig. 6). The 16-site silicon probes record voltage through the depth of the neocortex and allow calculation of CSDs that are displayed as colour contour plots (current sinks are red, sources are blue and zero is green). This reveals the laminar current flow through the neocortex during the discharges generated by neocortical disinhibition. Application of these methods *in vitro* has important advantages, for example it enables the experimenter to ascertain the exact location of the 16-site probe and allowing the probe to be repositioned as required.

Figure 6 shows a CSD analysis corresponding to a spontaneous discharge produced by disinhibition (BMI+CGP) in the granular cortex (left panel). As indicated above the discharges that originate in the granular cortex do not produce 10 Hz oscillations. Subsequently, the 16-site silicon probe was moved to the agranular neocortex in the same slice. In this slice a lesion was made between the granular and agranular regions to avoid communication between these two parts of the slice. The lesion was made by applying constant current through a 16-site silicon probe (1 mA DC, 20 s). The effectiveness of the lesion was demonstrated by using a stimulating electrode to evoke activity in one part of the slice and recording on the other part (Fig. 6, left photomicrograph). As shown in Fig. 6 (right panel) the probe located in the agranular neocortex of the same slice revealed discharges with 10 Hz oscillations caused by disinhibition (BMI+CGP). In general, the CSD analyses from the agranular cortex were very different from those obtained in the granular cortex reflecting both functional and architectural differences. Briefly, in the granular cortex the discharges consisted of a current sink that originates in the middle of layer VI with a corresponding current source in layer IV. This current sink propagates upward into layer V–IV, and is followed by a sink in upper layers II–III. The propagating sink within layer V–IV had a corresponding source in layer VI, while the sink propagating into the upper layers II–III had a corresponding current source in layers I–II (see Fig. 6, left panel). The wave component of the discharge was associated with two large current sources in layers V and III (Fig. 6, left panel). The layer V source had a corresponding sink in layer VI, while the layer III source had a corresponding sink above in layer I–II. Multi-unit activity recorded through the depth of the neocortex with the 16-channel probes showed that neuronal firing follows the direction of the current sink and spreads from layer VI to the upper layers (not shown; the details of current flow associated with spontaneous discharges in the granular neocortex will be dealt with in a different study).

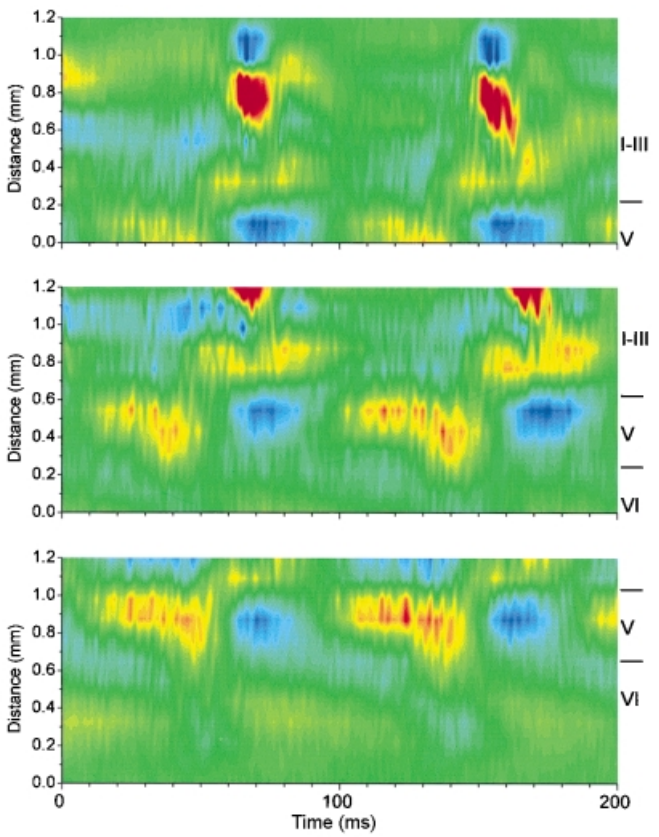

Figure 8. Close-up of CSD analysis corresponding to a 10 Hz oscillation

The CSD analyses are close-ups of those shown in Fig. 7 during BMI+CGP35348 (560–760 ms in Fig. 7). For comparison between the different CSD analyses they are aligned by the layer V current source, which is visible in all of them.

Figure 7 shows CSD analyses derived from spontaneous discharges in the agranular neocortex of another slice in the presence of BMI, before (middle panels) and during (right panels) the application of CGP35348 (500 μM). The probe was placed at different distances with respect to the pia mater in order to determine the locations of the sinks and sources (left panels). In agranular cortex layer IV is virtually inexistent and mixed with layer III, and layer V is larger than in the granular cortex (Zilles, 1985). The initial negative spike component of the discharge was not significantly affected by $GABA_B$ receptor blockade (Fig. 7). The initial negative spike in the agranular neocortex consisted of a current sink that originates in upper layer VI and spreads to lower layer V (Fig. 7; see also Fig. 6, right panel). This sink has a corresponding source in lower layer VI. The sink then jumps into layer II–III propagating upward, with a corresponding source in layer I–II (Fig. 7). Later another sink originates in lower layer III, which has a corresponding source in upper layer V. This sink propagates slowly into layer II generating a large sink in that layer, which has a corresponding source above it in layer I. The wave component of the discharge in the agranular cortex was associated with a large current source in layer III, which has a corresponding sink in layer V (Fig. 7). The layer III source spreads into layer II generating another source there that has a corresponding

current sink in layer I. In addition, a smaller source is also apparent in the border of layer VI and V, which has a corresponding sink in lower layer VI (Fig. 7). It is from these late sinks–sources associated with the wave component of the discharge that the 10 Hz oscillations are generated during disinhibition (Fig. 7). The 10 Hz oscillations consist of a series of current sinks in layers VI, V and II–III. The sinks in layer II–upper III are the strongest associated with the oscillation, and they have a corresponding source in layer I. Thus, the oscillation is most strongly expressed in the upper layers. However, the sinks in layer V invariably precede those in layer II–III. This is apparent in Fig. 8, which shows a close-up of the CSD analyses from Fig. 7 (right panels, 560–760 ms) during disinhibition (BMI+CGP). The two cycles of the oscillation shown in Fig. 8 reveal a sink in layer V followed by one in lower layer III and latter the upper layer large current sinks. Thus, although the oscillation is strongly expressed in the upper layers this activity may be driven by lower layer activity. Moreover, the sink in layer VI seems to be associated with a source in layer V that follows the initial layer V sink. This layer V source increases in amplitude with each cycle of the oscillation until the oscillation stops (Fig. 7, right panels). The present results indicate that the 10 Hz oscillation caused by disinhibition in the agranular neocortex is expressed strongly in the upper layers (I–III) with activity preceding in the lower layers.

The last experiment tested the effect of blocking AMPA receptors on the current flow generated in the agranular neocortex during 10 Hz oscillations. In particular we wanted to see if the current sinks observed in the lower layers that seem to precede the upper layer sinks might persist after AMPA receptor blockade. If some current sinks persisted it would suggest that lower layer neurons continue to discharge intrinsically after block of AMPA receptors. Figure 9 shows a CSD analysis during application of BMI, BMI+CGP and subsequent addition of CNQX (2 μM). In every experiment ($n = 6$) the result was the same, all current flow associated with the oscillation in all layers was abolished after blocking AMPA receptors. The current flow in the presence of CNQX reverted to the flow observed in the presence of BMI alone. This result supports the notion that recurrent synaptic activity mediated by AMPA receptors generates the 10 Hz oscillations caused by disinhibition in neocortex. Thus, the intrinsic membrane properties of cortical neurons in agranular neocortex seem useless to generate 10 Hz oscillations without recurrent synaptic activity mediated by AMPA receptors.

DISCUSSION

The present study found that application of a $GABA_A$ receptor antagonist in neocortical slices transforms spontaneous slow oscillations into large amplitude ~0.1 Hz discharges that consist of a large negative spike followed by a positive wave. Further block of $GABA_B$ receptors transforms the discharge by adding three to fifteen low amplitude negative spikes that ride on the positive wave and form a rhythmic ~10 Hz (7–14 Hz)

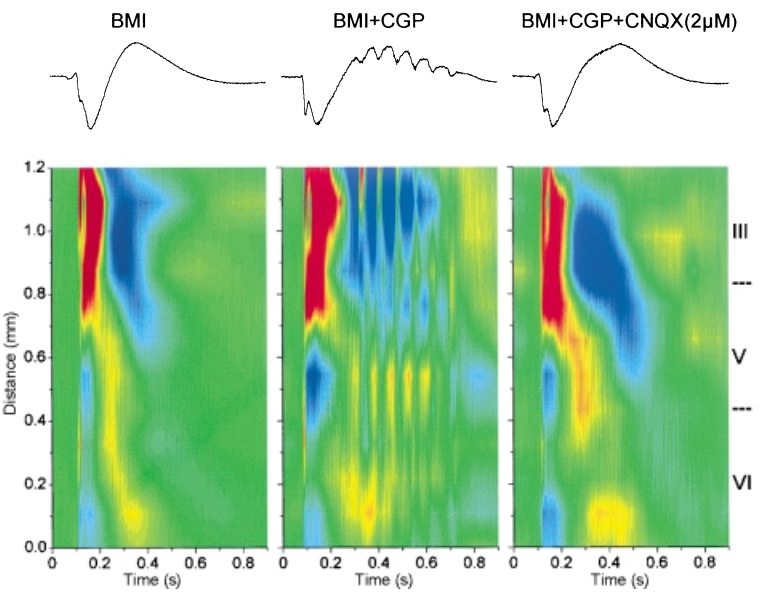

Figure 9. Effect of 2 μM CNQX on 10 Hz oscillations measured with CSD analysis in the agranular neocortex

Upper panel, traces corresponding to the CSD analyses shown below recorded from one of the sites on the 16-channel probe. Lower panel, CSD analysis corresponding to spontaneous discharges generated in the agranular cortex during application of BMI, BMI+CGP35348 and BMI+CGP35348+CNQX (2 μM). Note the abolishment of all current flow associated with the oscillation after application of CNQX.

neocortical oscillation. The 10 Hz oscillation caused by disinhibition is highly region specific and is generated only in frontal agranular regions of neocortex, such as the primary motor cortex, but not in granular neocortex, such as the primary somatosensory cortex. Pharmacological manipulations, CSD analyses and intracellular recordings indicate that blocking $GABA_B$ receptors in agranular neocortex unmasks recurrent synaptic connections mediated by AMPA receptors that results in the generation of the 10 Hz oscillations and their strong expression in the upper layers.

Effect of disinhibition in neocortical slices: region specificity

In the present study, we used slices from adults that produce spontaneous slow wave oscillations under control conditions. Application of a $GABA_A$ receptor antagonist to these slices resulted in the production of spontaneous spike–wave discharges that recur at ~0.1 Hz following the frequency of slow oscillations. Thus, the activity generated in the present study *in vitro* resembles the activity we described previously *in vivo* after $GABA_A$ receptor blockade in the neocortex of rodents (Castro-Alamancos, 2000). The present study in slices also found that simultaneous application of $GABA_A$ and $GABA_B$ receptor antagonists resulted in the induction of spontaneous discharges that produce a ~10 Hz oscillation. This was also previously observed *in vivo* in the primary motor cortex of rodents (Castro-Alamancos, 2000). Here we describe that the generation of these oscillations is exclusive of certain neocortical areas, including the agranular frontal neocortex, but not the granular neocortex. This indicates that specific regions of neocortex have the intrinsic capability to trigger certain forms of oscillatory activity, which is absent in other regions. Neocortex is extensively subdivided into areas of anatomical and functional specialization (Creutzfeldt, 1995), but little is known about the specialization of cellular physiology across areas. For example, theta-burst stimulation applied to layer V–IV produces long-term potentiation (LTP) in layer III of granular cortex, while the same procedure in the agranular neocortex is ineffective unless inhibition is suppressed (Castro-Alamancos *et al.* 1995). Also, electrical stimulation of the ventrolateral nucleus of the thalamus which projects to the agranular primary motor cortex produces augmenting responses consisting of progressively enhanced cortical responses when stimuli are delivered at between 7 and 14 Hz (Castro-Alamancos & Connors, 1996*a*), which is the frequency range of the oscillations described in the present study. In contrast, stimulation of the ventroposterior lateral nucleus projecting to the granular primary somatosensory cortex of rats at these same frequencies does not generate augmenting responses, but decrementing responses, unless higher stimulation currents are used (Castro-Alamancos & Connors, 1996*a*) which probably trigger intrathalamic mechanisms that can also generate augmenting responses (Bazhenov *et al.* 1998; Timofeev & Steriade, 1998; Castro-Alamancos & Calcagnotto, 1999, 2001). Moreover, augmenting responses are obtained in isolated neocortical slices of rats by stimulating locally and recording in layer V of the agranular region (Castro-Alamancos & Connors, 1996*b*). However, interspecies differences could be very important in this regard because the granular cortex of cats also produces augmenting responses even after thalamic lesions (Steriade & Morin, 1981), suggesting that the results obtained in the present study with rodents may not be directly applicable to cats. In fact, although a mapping study of different cortical areas has not been performed in cats, fast-runs caused by BMI, which are similar to the 10 Hz oscillations, have been described in the granular cortex of cats, e.g. visual cortex (Neckelmann *et al.* 1998).

Taken together, these data suggest that the agranular neocortex has an intrinsic network, which is tuned to the 7–14 Hz frequency range. What is the cause of this frequency preference? The answer to this question deserves further exploration. However, there are several possibilities. First, a group of cells may have the intrinsic property to oscillate at this frequency range. Second, the agranular neocortex may be wired in such a way that it favours the generation of oscillations at this frequency range. Finally, both the presence of cells with specific intrinsic properties and the synaptic organization of the agranular cortex may be responsible for the generation of the oscillation. Interestingly, there is evidence that the neocortex of rodents contains neurons that are able to intrinsically oscillate at about 7–14 Hz (Agmon & Connors, 1989; Silva *et al.* 1991). Although a comparison between neocortical areas has not been performed, the agranular neocortex does contain these neurons (Castro-Alamancos & Connors, 1996*b*). At the morphological level granular and agranular areas are very distinct, after all this is how areas are distinguished. The granular area lies lateral and posterior to the agranular area, and is named for the small, dense neurons of its layer IV. The agranular area lacks a dense layer IV, having instead a thick layer V (Donoghue & Wise, 1982; Zilles, 1985). Thus, there are ample differences between both neocortical regions that could explain the distinct effects of disinhibition observed in the present study. One scenario could be the presence of a cell population in the agranular cortex that is sensitive to $GABA_B$ receptors, which is absent in the granular cortex and is critical for the generation of 10 Hz oscillations. Indeed, $GABA_B$ receptors seem to be most abundant in frontal areas of neocortex (Bowery *et al.* 1987). The sensitivity to $GABA_B$ receptors in the agranular neocortex could be at the level of dendrites or presynaptic terminals.

In the case of dendrites, a current might be unmasked when $GABA_B$ receptors are blocked that makes the neuron oscillate at 10 Hz (Scanziani, 2000). Alternatively, blocking $GABA_B$ receptors may eliminate a presynaptic depression caused by activation of presynaptic $GABA_B$ hetero-receptors located on glutamatergic terminals (Isaacson *et al.* 1993). In this case, GABA released during the first large amplitude discharge acting on presynaptic $GABA_B$ receptors would mask the recurrent excitatory connections between populations of neurons. This presynaptic inhibition would impede the synaptic coupling needed to generate the oscillations. Blocking $GABA_B$ receptors would eliminate the presynaptic depression of glutamate release and allow the generation of the oscillations. The present study supports this hypothesis because the oscillations generated by disinhibition are completely eliminated by blocking a specific glutamate receptor the AMPA receptor (see below).

Involvement of glutamate receptors in 10 Hz oscillations

In the present study, we investigated the role of the three types of glutamate receptors (metabotropic, NMDA and non-NMDA receptors) in generating the 10 Hz oscillations. Glutamate receptors must play a critical role in the generation of the 10 Hz oscillations because the other major source of neurotransmission in the neocortex (GABA) is blocked during the oscillations. We found that metabotropic glutamate receptors have little involvement in the generation of these discharges. Blocking these receptors simply increased the oscillation slightly suggesting that the large amount of glutamate released during a discharge tends to decrease further glutamate release via metabotropic autoreceptors. This is plausible since the glutamatergic synapses of neocortex are depressed by activation of metabotropic glutamate receptors (Burke & Hablitz, 1994*b*) and so are epileptic discharges (Burke & Hablitz, 1994*a*). In contrast with the effects of metabotropic antagonists, blocking NMDA receptors had significant effects on the 10 Hz oscillations induced in agranular neocortex during disinhibition. Thus, blocking NMDA receptors reduced the amplitude of the oscillation. However, the oscillation was not abolished, instead the frequency was enhanced so that it was transformed from a 10–15 Hz oscillation to a 15–25 Hz oscillation. This indicates that during the oscillation NMDA receptors are strongly activated, and serve to shape the form of the oscillation. In particular, NMDA receptors seem to be critically involved in setting the frequency of the oscillation. In the hippocampus, afterdischarges similar to the 10 Hz oscillations of agranular neocortex are abolished by NMDA receptor blockade (Lee & Hablitz, 1990; Traub *et al.* 1993*b*, 1996). Thus, afterdischarges in the hippocampus and 10 Hz oscillations in the neocortex are mechanistically distinct. This is not surprising considering the great differences between the hippocampus and agranular neocortex. The 10 Hz oscillations are also distinct from those generated in neocortical slices by low-magnesium buffers, which are also completely abolished by NMDA receptor antagonists (Silva *et al.* 1991).

Since NMDA receptor block does not abolish the 10 Hz oscillations in the agranular neocortex, we reasoned that block of non-NMDA receptors should eliminate these oscillations. There are two types of non-NMDA receptors, kainate and AMPA. We found that a low dose of CNQX, which is selective for AMPA receptors, or a selective AMPA antagonist completely abolish the 10 Hz oscillations without affecting the initial spike–wave discharge. This indicates that AMPA receptors are critically involved in the generation and/or expression of the 10 Hz oscillations. There are several possible ways in which AMPA receptors may be involved. They may simply express the oscillation, which is generated intrinsically by a population of cells, or they may interconnect networks of cells from which the oscillation emerges. In both cases, blocking these receptors would eliminate the oscillation. However, if the former were the case individual cells that intrinsically discharge at ~10 Hz should continue to produce the oscillation during AMPA receptor block, but this was not the case. Intracellular recordings from layer V neurons that intrinsically burst at these frequencies stop generating the 10 Hz oscillations when AMPA receptors are blocked. Moreover, CSD analysis confirmed that all current flow in every layer associated with the 10 Hz oscillations was abolished when AMPA receptors are blocked. Thus, AMPA receptors are crucial for generating the 10 Hz oscillations. The importance of AMPA receptors is further supported by the observation that NMDA receptors alone can sustain the initial large amplitude spike–wave discharges after AMPA receptors are blocked, but not the 10 Hz oscillations (see Figs 4, 5 and 6). Consequently, if the 10 Hz oscillations were generated at all during AMPA receptor blockade then NMDA receptors should be able to express them. Instead, the results show that during AMPA receptor block there is not even a hint of the 10 Hz oscillations, indicating that when AMPA receptors are blocked the 10 Hz oscillations are not generated.

Silicon probes in slices

An important contribution of the present study is the application of 16-channel silicon probes in neocortical slices so that cortical activities can be studied *in vitro* with high temporal and spatial resolution. This method has a major advantage over its application *in vivo*; the position of the probe can be visualized and changed as required. With the application of these methods we visualized the spatio-temporal characteristics of the activities generated by disinhibition in the granular and agranular neocortex.

In the granular neocortex, the spike component in a discharge consists of a current sink originating in layer VI that spreads into layer V–IV jumping then into the upper layers. The wave component of the discharge consisted of two large current sources in layers V and III, with corresponding sinks in layer VI and I–II, respectively. The spike–wave discharges in the agranular neocortex were more complex and very different from those in granular neocortex. The spike component in the agranular neocortex consisted of a current sink that originates in upper layer VI and spreads to lower layer V, followed by a sink in layer II–III that propagates upward rapidly and another sink also in lower layer III that propagates upward much more slowly. The wave component of the discharge was associated with a large current source in layers II–III. The 10 Hz oscillations were strongly expressed in the upper layers with large current sinks in layers II–III and corresponding sources in layer I. However, current sinks were also observed in layer V prior to the upper layer sinks suggesting that the activity in the lower layers may drive the expression of the oscillation in the upper layers, as was shown previously *in vivo* (Castro-Alamancos, 2000).

How are 10 Hz oscillations generated?

The present study provides several important findings toward elucidating the mechanisms responsible for generating the 10 Hz oscillations. First, it provides an *in vitro* model of the 10 Hz oscillations that highly resembles the same activity obtained *in vivo* under the same conditions (i.e. disinhibition). Second, 10 Hz oscillations are region specific. They are mainly produced in the agranular frontal neocortex, suggesting that $GABA_B$ receptor-sensitive cells present in agranular neocortex, but absent in other neocortical areas, generate the 10 Hz oscillations. Third, pharmacological manipulations demonstrate that AMPA receptors are critical for 10 Hz oscillations, while other glutamate receptors are not. Fourth, neurons that can intrinsically fire at the frequency of these oscillations will not do so in response to a spontaneous discharge when AMPA receptors are blocked indicating a critical role for synaptic recurrent activity in the generation of these oscillations. Fifth, the upper layers primarily express the oscillations perhaps driven by lower layer activity. These results taken together suggest the following scenario. In the agranular neocortex blocking $GABA_B$ receptors unmasks recurrent synaptic connections mediated by AMPA receptors, which are suppressed by GABA released during the initial spike–wave discharge acting on presynaptic $GABA_B$ receptors. The unmasked recurrent activity coupled perhaps with the intrinsic firing of cortical cells generates the 10 Hz oscillations. One important question is: what cell population that has $GABA_B$ receptors and is present in the agranular neocortex, but not in granular neocortex, is crucial for the generation of these oscillations? The present *in vitro* model should be useful to define them.

REFERENCES

Agmon, A. & Connors, B. W. (1989). Repetitive burst-firing neurons in the deep layers of mouse somatosensory cortex. *Neuroscience Letters* **99**, 137–141.

Bazhenov, M., Timofeev, I., Steriade, M. & Sejnowski, T. J. (1998). Cellular and network models for intrathalamic augmenting responses during 10-Hz stimulation. *Journal of Neurophysiology* **79**, 2730–2748.

Bowery, N. G., Hudson, A. L. & Price, G. W. (1987). GABAA and GABAB receptor site distribution in the rat central nervous system. *Neuroscience* **20**, 365–383.

Bragin, A., Csicsvari, J., Penttonen, M. & Buzsaki, G. (1997*a*). Epileptic afterdischarge in the hippocampal-entorhinal system: current source density and unit studies. *Neuroscience* **76**, 1187–1203.

Bragin, A., Penttonen, M. & Buzsaki, G. (1997*b*). Termination of epileptic afterdischarge in the hippocampus. *Journal of Neuroscience* **17**, 2567–2579.

Burke, J. P. & Hablitz, J. J. (1994*a*). Metabotropic glutamate receptor activation decreases epileptiform activity in rat neocortex. *Neuroscience Letters* **174**, 29–33.

Burke, J. P. & Hablitz, J. J. (1994*b*). Presynaptic depression of synaptic transmission mediated by activation of metabotropic glutamate receptors in rat neocortex. *Journal of Neuroscience* **14**, 5120–5130.

Castro-Alamancos, M. A. (1999). Neocortical synchronized oscillations induced by thalamic disinhibition *in vivo*. *Journal of Neuroscience* **19**, RC27.

Castro-Alamancos, M. A. (2000). Origin of synchronized oscillations induced by neocortical disinhibition *in vivo*. *Journal of Neuroscience* **20**, 9195–9206.

Castro-Alamancos, M. A. & Calcagnotto, M. E. (1999). Presynaptic long-term potentiation in corticothalamic synapses. *Journal of Neuroscience* **19**, 9090–9097.

Castro-Alamancos, M. A. & Calcagnotto, M. E. (2001). High-pass filtering of corticothalamic activity by neuromodulators released in the thalamus during arousal: *in vitro* and *in vivo*. *Journal of Neurophysiology* **85**, 1489–1497.

Castro-Alamancos, M. A. & Connors, B. W. (1996*a*). Spatiotemporal properties of short-term plasticity sensorimotor thalamocortical pathways of the rat. *Journal of Neuroscience* **16**, 2767–2779.

Castro-Alamancos, M. A. & Connors, B. W. (1996*b*). Cellular mechanisms of the augmenting response: short-term plasticity in a thalamocortical pathway. *Journal of Neuroscience* **16**, 7742–7756.

Castro-Alamancos, M. A., Donoghue, J. P. & Connors, B. W. (1995). Different forms of synaptic plasticity in somatosensory and motor areas of the neocortex. *Journal of Neuroscience* **15**, 5324–5333.

Connors, B. W. (1984). Initiation of synchronized neuronal bursting in neocortex. *Nature* **310**, 685–687.

Creutzfeldt, O. D. (1995). *Cortex Cerebri: Performance, Structural and Functional Organization of the Cortex*. Oxford University Press, UK.

Donoghue, J. P. & Wise, S. P. (1982). The motor cortex of the rat: cytoarchitecture and microstimulation mapping. *Journal of Comparative Neurology* **212**, 76–88.

Gloor, P., Quesney, L. F. & Zumstein, H. (1977). Pathophysiology of generalized penicillin epilepsy in the cat: the role of cortical and subcortical structures. II. Topical application of penicillin to the cerebral cortex and to subcortical structures. *Electroencephalography and Clinical Neurophysiology* **43**, 79–94.

Gutnick, M. J., Connors, B. W. & Prince, D. A. (1982). Mechanisms of neocortical epileptogenesis *in vitro*. *Journal of Neurophysiology* **48**, 1321–1335.

Hablitz, J. J. (1984). Picrotoxin-induced epileptiform activity in hippocampus: role of endogenous *versus* synaptic factors. *Journal of Neurophysiology* **51**, 1011–1027.

Hablitz, J. J. (1987). Spontaneous ictal-like discharges and sustained potential shifts in the developing rat neocortex. *Journal of Neurophysiology* **58**, 1052–1065.

Hablitz, J. J. & Sutor, B. (1990). Excitatory postsynaptic potentials in rat neocortical neurons *in vitro*. III. Effects of a quinoxalinedione non-NMDA receptor antagonist. *Journal of Neurophysiology* **64**, 1282–1290.

Isaacson, J. S., Solis, J. M. & Nicoll, R. A. (1993). Local and diffuse synaptic actions of GABA in the hippocampus. *Neuron* **10**, 165–175.

Lee, W. L. & Hablitz, J. J. (1990). Effect of APV and ketamine on epileptiform activity in the CA1 and CA3 regions of the hippocampus. *Epilepsy Research* **6**, 87–94.

Lerma, J., Paternain, A. V., Rodriguez-Moreno, A. & Lopez-Garcia, J. C. (2001). Molecular physiology of kainate receptors. *Physiological Reviews* **81**, 971–998.

Matsumoto, H. & Ajmone-Marsan, C. (1964). Cortical cellular phenomena in experimental epilepsy: interictal manifestations. *Experimental Neurology* **9**, 286–304.

Miles, R., Wong, R. K. & Traub, R. D. (1984). Synchronized afterdischarges in the hippocampus: contribution of local synaptic interactions. *Neuroscience* **12**, 1179–1189.

Neckelmann, D., Amzica, F. & Steriade, M. (1998). Spike-wave complexes and fast components of cortically generated seizures. III. Synchronizing mechanisms. *Journal of Neurophysiology* **80**, 1480–1494.

Ralston, B. L. (1958). The mechanism of transition of interictal spiking foci into ictal seizure discharges. *Electroencephalography and Clinical Neurophysiology* **10**, 217–232.

Sanchez-Vives, M. V. & McCormick, D. A. (2000). Cellular and network mechanisms of rhythmic recurrent activity in neocortex. *Nature Neuroscience* **3**, 1027–1034.

Scanziani, M. (2000). GABA spillover activates postsynaptic GABA(B) receptors to control rhythmic hippocampal activity. *Neuron* **25**, 673–681.

Silva, L. R., Amitai, Y. & Connors, B. W. (1991). Intrinsic oscillations of neocortex generated by layer 5 pyramidal neurons. *Science* **251**, 432–435.

Somogyi, P., Tamas, G., Lujan, R. & Buhl, E. H. (1998). Salient features of synaptic organisation in the cerebral cortex. *Brain Research. Brain Research Reviews* **26**, 113–135.

Steriade, M., Amzica, F. & Contreras, D. (1996). Synchronization of fast (30–40 Hz) spontaneous cortical rhythms during brain activation. *Journal of Neuroscience* **16**, 392–417.

Steriade, M., Amzica, F., Neckelmann, D. & Timofeev, I. (1998). Spike-wave complexes and fast components of cortically generated seizures. II. Extra- and intracellular patterns. *Journal of Neurophysiology* **80**, 1456–1479.

Steriade, M. & Contreras, D. (1998). Spike-wave complexes and fast components of cortically generated seizures. I. Role of neocortex and thalamus. *Journal of Neurophysiology* **80**, 1439–1455.

Steriade, M. & Morin, D. (1981). Reticular influences on primary and augmenting responses in the somatosensory cortex. *Brain Research* **205**, 67–80.

Steriade, M., Nunez, A. & Amzica, F. (1993). A novel slow (< 1 Hz). oscillation of neocortical neurons *in vivo*: depolarizing and hyperpolarizing components. *Journal of Neuroscience* **13**, 3252–3265.

Timofeev, I. & Steriade, M. (1998). Cellular mechanisms underlying intrathalamic augmenting responses of reticular and relay neurons. *Journal of Neurophysiology* **79**, 2716–2729.

Traub, R. D., Borck, C., Colling, S. B. & Jefferys, J. G. (1996). On the structure of ictal events *in vitro*. *Epilepsia* **37**, 879–891.

Traub, R. D., Jefferys, J. G. & Miles, R. (1993*a*). Analysis of the propagation of disinhibition-induced after-discharges along the guinea-pig hippocampal slice *in vitro*. *Journal of Physiology* **472**, 267–287.

Traub, R. D., Miles, R. & Jefferys, J. G. (1993*b*). Synaptic and intrinsic conductances shape picrotoxin-induced synchronized after-discharges in the guinea-pig hippocampal slice. *Journal of Physiology* **461**, 525–547.

Zilles, K. (1985). *The Cortex of the Rat.* Springer-Verlag, Berlin.

Acknowledgements

Multichannel silicon probes were provided by the University of Michigan Center for Neural Communication Technology sponsored by NIH NCRR. The Medical Research Council of Canada, Natural Sciences and Engineering Council of Canada, Fonds de la Reserche en Sante du Quebec, Canadian Foundation for Innovation and Savoy Foundation, supported this research. We also thank Novartis for providing CGP35348 and IVAX Pharmaceuticals for providing GYKI53655.